Defects and Dark Current in Organic Photovoltaics and Impacts on Device Physics

A Dissertation

Presented to

the Faculty of Natural Science and Mathematics

University of Denver

In Partial Fulfillment

of the Requirements for the Degree

Doctor of Philosophy

by

Xin Jiang

November 2013

Advisor: Sean Shaheen

PREVIEW

UMI Number: 3607657

All rights reserved

INFORMATION TO ALL USERS
The quality of this reproduction is dependent upon the quality of the copy submitted.

In the unlikely event that the author did not send a complete manuscript
and there are missing pages, these will be noted. Also, if material had to be removed,
a note will indicate the deletion.

UMI 3607657

Published by ProQuest LLC (2014). Copyright in the Dissertation held by the Author.

Microform Edition © ProQuest LLC.
All rights reserved. This work is protected against
unauthorized copying under Title 17, United States Code

ProQuest LLC.
789 East Eisenhower Parkway
P.O. Box 1346
Ann Arbor, MI 48106 - 1346

PREVIEW

©Copyright by Xin Jiang, 2013

All Rights Reserved

PREVIEW

Author: Xin Jiang
Title: Defects and Dark Current in Organic Photovoltaics and Impacts on device physics
Advisor: Sean Shaheen
Degree Date: November 2013

Abstract

In this dissertation, we discussed the shape, energy level and density of defects in Organic Photovoltaic (OPV) devices by both theoretical and experimental methods. The energy band structure and intrinsic junctions of general standard and inverted OPV devices are investigated in detail. Transportation of separated holes and electrons in both structures are well analyzed. In chapter II, we developed a Monte-Carlo model to simulate charge transport process in organic materials. Marcus theory is applied to calculate the carrier transfer rate to build up hopping process in ideal lattices. Results of this model showed several properties of carriers regarding mobility, reorganization energy and Poole-Frenkel behavior. Time-of-Flight (TOF) measurement is simulated by our Monte-Carlo model. Four typical phases of TOF are fitted in the simulation, corresponding well to the experiment data. In chapter III, we introduced Impedance Spectroscopy as a useful technique to examine overall electronic component and internal structure. Geometric capacitance and depletion regions are found to describe the equivalent circuit of OPV. Another section of this chapter showed that impedance data can be also used by Mott-Schottky analysis to calculate the doping density and built-in voltage of Schottky junction, which is widely considered existing in standard OPV devices. Degradation and lifetime studies are the major topics of chapter IV. We compared three devices within different thickness of active layers under different illumination intensity. Open-circuit voltage, short-circuit current and fill factor are deeply

PREVIEW

analyzed to explain the decrease of conversion efficiency during degradation process. In addition, we utilize a simple method to estimate the lifetime of free carriers. In chapter V, impedance spectroscopy is used to investigate the electronic structure of OPV devices, with the goal of understanding the role of defect states. Capacitance-voltage measurements in the temperature range of 77 - 300 K are carried out to determine the activation energy of trap states. Preliminary results show at least one type of defect state residing at 166 meV in standard blends of P3HT:PCBM. Furthermore we compared three different molecular weight of P3HT in both standard and inverted devices. The result shows that higher molecular weight provides deeper defects energy level, and the density of defects generated during fabrication is different for standard and inverted structures. In chapter VI, JV curve behavior, capacitor-voltage analysis and efficiency comparisons before annealing and after annealing are performed to conclude that a p-n junction is formed at the ZnO/P3HT interface in inverted devices. We also discussed the free carrier transportation in both structure and explain why annealing leads to different conversion efficiency changes. Finally the equivalent circuit is confirmed by agreement with the geometric capacitance, as well as the structure and transportation analysis discussed in rest of the dissertation.

PREVIEW

Table of Contents

PREVIEW

PREVIEW

List of Tables

PREVIEW

List of Figures

PREVIEW

PREVIEW

PREVIEW

PREVIEW

Chapter 1 Introduction

1.1 Motivation for OPV Study

Advancing renewable energy technologies is of critical importance to fulfilling the future energy needs for the planet. Solar energy is one of the most significant, due to easily obtained and unlimited sun power during daytime. Traditional study is concentrated on monocrystalline solar cells, especially silicon based. Although such devices are more efficient compared with other methods, the cost to make sufficient purity of silicon crystal is quite high, and the process consumes tremendous energy and produces significant hazardous waste.. Thin film photovoltaics were devised to reduce the cost of solar cells in lab, but the manufacture of such devices needs to be implemented in vacuum and is difficult to easily upscale and industrialize. Although recently thin film photovoltaics in the form of CdTe have done well on the marketplace, it is not clear if they can ever be scaled to become a major contributor to the world's energy flow. To overcome such disadvantages, Organic Photovoltaic (OPV) devices have become a new research field of solar energy, which is a promising low-cost technology that is approaching commercialization. Organic materials are far less inexpensive compared to silicon crystal. The methods of printing OPV devices at high speed on flexible substrates, or making devices by roll-to-roll processing are attractive projects for

PREVIEW

both research and industry fields. In all, we expect that OPV is a suitable balance between system cost and conversion efficiency.

Recently several institutes and research groups have efficiencies approaching 12%. Mitsubishi Chemical Group achieves 10% efficiency in a single-junction Organic device. By applying materials and a production technology different to those used for crystalline silicon-type cells, it has developed the world's first solution conversion type organic photovoltaic. Professor Yang Yang and his research team in UCLA fabricated a tandem polymer device having conversion efficiency of 10.6% [1], certificated by NREL in Feb. 2012. Heliatek also claimed to get 12.0 percentages efficiency as the world record until now. To date, this is the highest reported OPV efficiency and is based on a multijunction device utilizing small molecule and oligomer materials.

The long term goal of OPV field is to make 15%-20% efficiency devices by low-cost organic materials. Since the efficiency has not reached the ideal value for industrialization, lifetime is not a major topic in OPV research field until now, but we expect to optimize the durability to more than ten years. Many companies and research groups have fierce competition about the OPV conversion efficiency. The Company Helitatek in German is the leader of this year. However it cannot remain its honor for a long time, as the increasing growth rate of conversion efficiency shown in Fig. 1.1.

PREVIEW

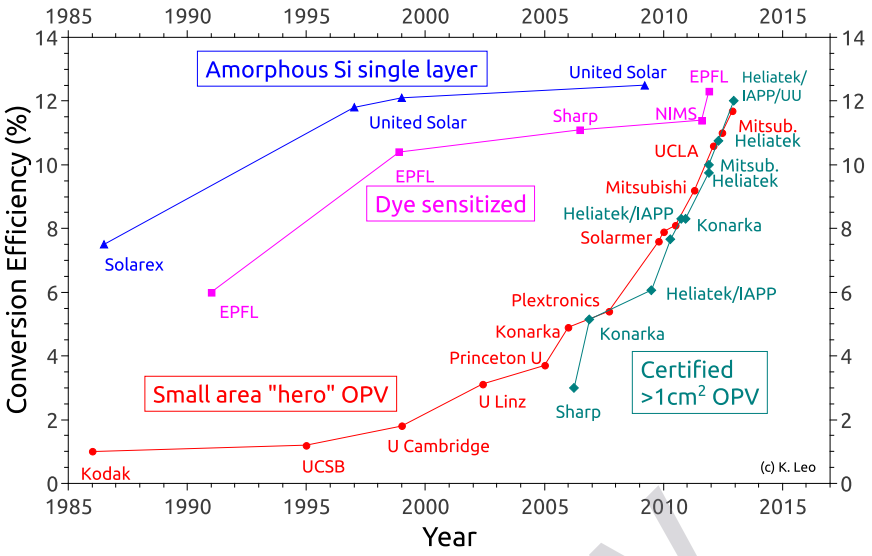

Figure 1.1. OPV power conversion efficiency world record chart.
http://www.orgworld.de/

PREVIEW

1.2 Characteristics of Photovoltaics

1.2.1 Equivalent Circuits

Several semiconductor books introduce the basic properties and simple equivalent circuit of solar cells [2, 3]. At short circuit condition, photocurrent generated by a solar cell under illumination is dependent on incident light.

$$J_{sc} = q \int b_s(\lambda)\, QE(\lambda)\, dx \quad (1.1)$$

where J_{sc} is recognized as short-circuit current density, $b_s(\lambda)$ is the photon flux (the incident power intensity), and $QE(\lambda)$ is the quantum efficiency of the device at a given wavelength. Generally devices at different wavelength have different conversion efficiency. Photons at a specific range of wavelengths, which provide sufficient energy to

overcome the intrinsic device's band gap, contribute to the short current that is expressed mathematically as integrating the product of the photon flux and quantum efficiency.

In dark, most solar cells perform as a diode, admitting charge transport through devices under forward bias and prohibiting conversely. The rectifying behavior is a feature of photovoltaic device, designed to choose material of suitable energy level to form junction, from where electron and hole are separated and driven to different directions. Current density through an ideal diode is expressed as,

$$J_{dark}(V) = J_0\left(e^{qV/k_BT} - 1\right) \quad (1.2)$$

Under illumination, photocurrent is generated in the solar cell and transport through the load. Electrically, we can describe the process and structure as a diode and a current source in parallel, representing the simple equivalent circuit of ideal device.

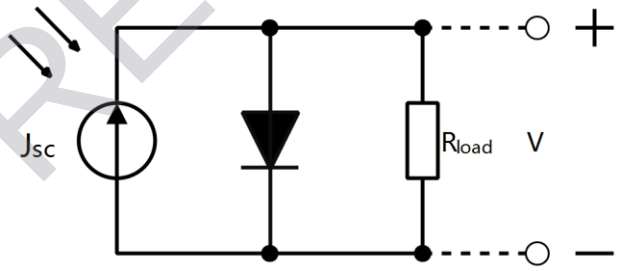

Figure 1.2. The simplest equivalent circuit for a photovoltaic device.

As shown in Fig. 1.2, the net current through R_{load} is the combination of J_{sc} generated by incident light and dark current through diode due to potential difference V on devices.

PREVIEW

$$I(V) = I_{sc} - I_{dark}(V) \quad (1.3)$$

$$V = IR_{load} \quad (1.4)$$

Considering net current through ideal diode without charge recombination contribution in depletion layer,

$$I = I_{sc} - I_o\left(e^{qV/k_BT} - 1\right) \quad (1.5)$$

where I_o is the saturation current. When the device does not connect any load, the potential difference reaches maximum value, open circuit voltage:

$$\begin{aligned} V_{oc} &= \frac{KT}{q}\ln\left(\frac{I_{sc}}{I_o} + 1\right) \\ &\approx \frac{KT}{q}\ln\left(\frac{I_{sc}}{I_o}\right) \end{aligned} \quad (1.6)$$

$I_{sc} \gg I_o$, Since reverse saturation current of most diodes in OPV devices is ignorable compared with short circuit current induced by invisible light.

In real solar cell devices, dissipation comes about from the resistance of contacts as well as leakage currents that shunt the device. Two parasitic resistances in series and in parallel are added into circuit to represent those effects (Fig. 1.3). Series resistance R_s comes from absorption materials, contact, connections and etc. It is a major cause for reduced current density. Leakage current through shunt resistance R_{sh} at the edges of cells, leads to poor rectifying property. Both dissipation mechanisms will lower the conversion efficiency.

PREVIEW

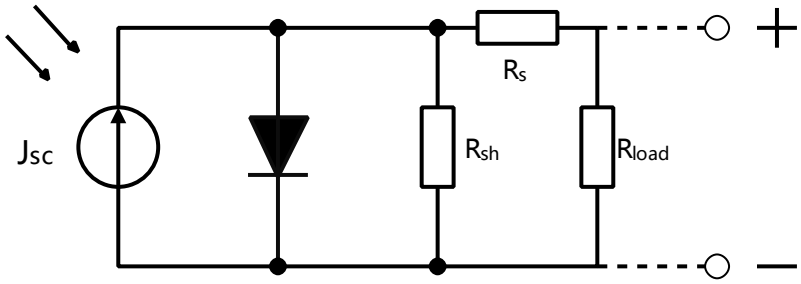

Figure 1.3. Equivalent circuit for a photovoltaic device including series dissipation and parallel leakage.

After R_s and R_{sh} are added into equivalent circuit, the net current through load is revised as

$$I = I_{sc} - I_o\left(e^{q(V+IR_s)/k_BT} - 1\right) - \frac{V+IR_s}{R_{sh}} \quad (1.7)$$

It is obvious that we expect R_s to be small and to R_{sh} be large to produce larger photocurrent.

PREVIEW

1.2.2 Parameters to Evaluate Efficiency

Several parameters are important to distinguish properties of solar cell. Output of one solar cell is in the range of voltage, from 0 to V_{oc}, current density from 0 to J_{sc}. The cell power density is determined by

$$P = JV \quad (1.8)$$

Generally we scan our devices by power supply and source measure units, in the range of bias voltage from some negative value to some positive value which should be

larger than V_{oc}. A series of current density and bias voltage in pair can be read from instrument. Note that those values are following Eq. 1.5 or Eq. 1.7 depended on ideal simplification or dissipation simplification. The plot of current versus bias is called J-V curve.

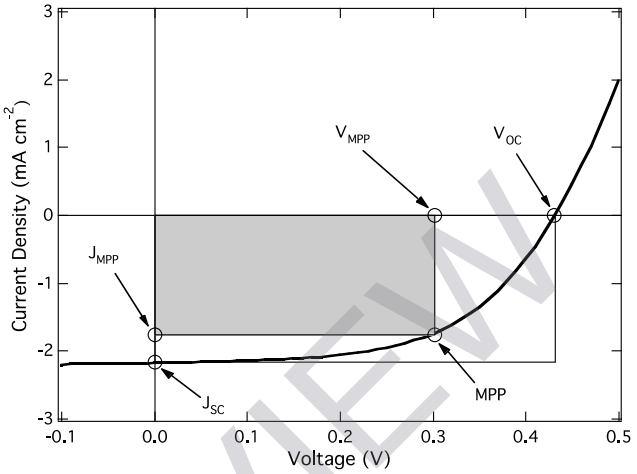

Figure 1.4. A typical J-V curve for a photovoltaic device.

Fig. 1.4 is a typical J-V cure plot. For one scan in the range of bias voltage from 0 to V_{oc}, maximum power density reaches at some point. This occurs at some voltage V_m with a corresponding current density J_m. We call it maximum power point (MPP), from which an important parameter named Fill factor (FF) is defined as

$$FF = \frac{J_m V_M}{J_{sc} V_{oc}} \quad (1.9)$$

We also define the efficiency as maximum power density over incident light power density,

PREVIEW

$$\eta = \frac{J_m V_m}{P_s} = \frac{J_{sc} V_{oc} FF}{P_s} \quad (1.10)$$

J_{sc}, V_{oc} and FF is determined by the internal characteristic of each device. They are the kernel parameters to calculate the efficiency. Relied on Eq. 1.7, lowering R_s or raising R_{sh} is of importance to achieve a great fill factor value.

Another issue is about how to achieve the maximum power point. An easy method is to add converters as intermediate circuits to assure the devices working near MMP.

Figure 1.5. Schematic diagram of connections of devices, the converter and , and the load.

PREVIEW

1.2.3 Ideal Efficiency

According to Eq. 1.5, power of one cell device is expressed as,

$$p = IV = I_{sc} V - I_o \left(e^{qv/kt} - 1 \right) V \quad (1.11)$$

Maximum efficiency is achieved when

$$\frac{dP}{dV} = \frac{d}{dV} (IV) = 0 \quad (1.12)$$

We define $\beta \equiv q/kT$ for simplification. I_m and V_m are the value of current and bias at maximum power point. As a result of Eq. 1.12,

$$I_{sc} - I_o\left(e^{\beta V_m} - 1\right) - I_o \beta V_m e^{\beta V_m} = 0 \quad (1.13)$$

Two exponential terms in the expression above are added together to determine the expression of V_m,

$$\begin{aligned} V_m &= \frac{1}{\beta}\ln\left(\frac{I_{sc}}{I_o} + 1\right) - \frac{1}{\beta}\ln\left(1 + \beta V_m\right) \\ &= V_{oc} - \frac{1}{\beta}\ln\left(1 + \beta V_m\right) \end{aligned} \quad (1.14)$$

We can also get the expression of I_m by combining Eq. 1.5 and Eq. 1.13.

$$I_m = I_o \beta V_m \exp\left(\beta V_m\right) \quad (1.15)$$

Therefore ideal efficiency is described in detail by inserting the expression of I_m into Eq. 1.10.

$$\eta = \frac{P_m}{P_s} = \frac{I_o \beta V_m^2 \exp\left(\beta V_m\right)}{P_s} \quad (1.16)$$

where V_m follows Eq. 1.14, and I_o is the saturation current of a general p-n junction, which is determined by intrinsic properties, like diffusion coefficient, carrier lifetime and energy gap E_g,

$$I_o = AqN_cN_v\left(\frac{1}{N_A}\sqrt{\frac{D_n}{\tau_n}} + \frac{1}{N_D}\sqrt{\frac{D_p}{\tau_p}}\right)\exp\left(\frac{-E_g}{kT}\right) \quad (1.17)$$

PREVIEW

Theoretically we can calculate the ideal efficiency, after we measure properties of diode behavior cells in dark.

Considering all the equations in this section, some relationships among those parameters need to be discussed in detail.

$$E_g \uparrow \quad \rightarrow \quad I_o \downarrow \quad \rightarrow \quad I \uparrow \ \& \ V_{oc} \uparrow \quad \rightarrow \quad V_m \uparrow$$

Eq. 1.17 determines the relationship between E_g and I_o. Following Eq. 1.5 and Eq. 1.6, we can straightforward conclude that net current (I) and open circuit voltage (V_{oc}) increase due to enhancement of E_g. V_m, which is determined by Eq. 1.14, and increase gradually by E_g, as a result of those recursive relationships. Hence the monotonicity of I_o and V_m is adverse. Based on the expression Eq. 1.16, certain energy gap would lead to optimal conversion efficiency theoretically. When we design a solar device, what is the suitable energy gap to achieve sufficient efficiency, whether the gap is too extreme for exciton separation, those details should be carefully considered.

However, practical efficiency is lowered sharply by several factors. Firstly series resistance and leakage resistance cannot be ignored. Secondly dark current is contributed more by recombination current in depletion region for real solar cell. Expression of dark current through diode is replaced as,

$$I_{dark} = I_o^{'} \left[\exp\left(\frac{qV}{nkT}\right) - 1 \right] \tag{1.18}$$

PREVIEW

where n is in the range of 1 to 2 in real situations, since it is equal to 1 for ideal p-n junction, while the value is 2 for pure recombination current. The actual efficiency is lowered, as the output current is reduced within larger value of n.

1.3 Structure and Physics of Organic Photovoltaic Devices

Several reviews [2, 4] have discussed the complete process regarding how photon are absorbed by conjugated materials to generate excitons; excitons diffuse to interface to provide opportunity for separation of holes and electron; and free carriers travel through active layer to be collected at electrodes. We do not discuss here the more complicated but more accurate scenarios that have more recently been discussed in the literature, which depend on charge transfer state formation at the donor-acceptor interface and on more complicated morphologies than simply a mixture of pure donor and pure acceptor domains. Fig. 1.6 shows a standard OPV devices' structure for this discussion. First incident light travels though the bottom layer, which is a transparent substrate, typically made by glass. Second layer is some effective transparent conducting electrode, such as Indium Tin Oxide (ITO). ITO is historically one of the best-performing transparent, highly conductive and solid materials, wildly used as electrode in OPV and OLED devices. PEDOT:PSS plays role as a buffering layer to provide intermediate work function between ITO and active layer. It has high transparency in visible range, considered as an excellent conducting and electro-optical polymer. The most important layer is the active layer that is made by blends of donor and acceptor materials, creating

PREVIEW

bulk D/A heterojunction. The general method of fabricating such layer is to make mixture solution of donor and acceptor at a proper ratio, and spin-cast on ITO substrate. In Fig. 1.6, active layer is the thin red layer between metal electrode and ITO. The morphology of the donor and acceptor blend is determined by several factors, such as spin-cast speed, composition of two materials, solution concentration, and annealing treatmet; however, the final morphology of most OPV devices is amorphous as the shape inside the active layer of Fig. 1.6 depicts. Such structure provides many "paths" for charge transport between anode and cathode, as well as tremendous junctions between donor and acceptor molecules at "everywhere" inside bulk layer. Generally, only one material (donor or acceptor) in active layer is conjugated polymer, which has great capability to absorb visible light. Typical OPV devices are made by p-type conjugated polymer and n-type fullerene derivatives, which as excellent electron acceptors. The top layer is metal electrode selected by work function. In Chapter VI, structure of standard and inverted device will be well discussed, elaborating how the work function of metal electrode affects performance.

PREVIEW

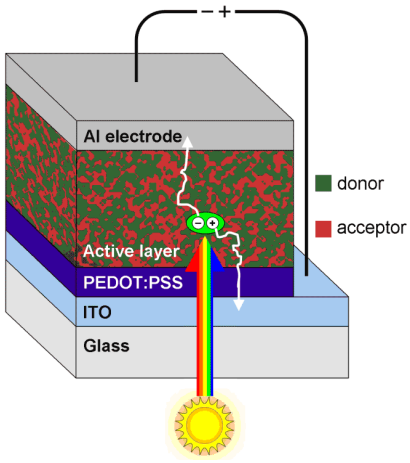

a)